Current Oscillatory Phenomena Based on Redox Reactions at a Hanging Mercury Drop Electrode (HMDE) in Dimethyl Sulfoxide

Md. Mominul Islam, Takeyoshi Okajima, and Takeo Ohsaka*

Department of Electronic Chemistry, Interdisciplinary Graduate School of Science and Engineering, Tokyo Institute of Technology, Mail Box G1-5, 4259 Nagatsuta, Midori-ku, Yokohama 226-8502, Japan

Received: August 9, 2004

A systematic and comprehensive study on cyclic voltammetric anodic current oscillation (CVACO) at a hanging mercury drop electrode (HMDE) was carried out for the redox reactions of molecular oxygen (O_2), nitrobenzene (NB), 1,4-dinitrobenzene (DNB), benzoquinone (BQ), 2,3,5,6-tetramethylbenzoquinone (TMBQ), benzophenone (BP), azobenzene (AB), 2,1,3-benzothiadiazole (BTD), 7,7,8,8-tetracyanoquinodimethane (TCNQ), methyl viologen dichloride (MV^{2+}), and tris(2,2′-bipyridine)ruthenium(II) dichloride [$Ru(bpy)_3^{2+}$] in dimethyl sulfoxide (DMSO) solutions containing 0.1 M tetraethylammonium perchlorate (TEAP). From the electrocapillary curve (ECC) obtained using a dropping mercury electrode as well as the capacitance versus potential curves measured using electrochemical impedance technique, the value of the potential of zero charge (PZC) was estimated to be −0.27 V versus Ag|AgCl|NaCl (sat.) in a DMSO solution containing 0.1 M TEAP. CVACO was found to occur only for the redox couples (i.e., $BP^0/BP^{\bullet-}$, $O_2{}^0/O_2{}^{\bullet-}$, $AB^0/AB^{\bullet-}$, $Ru(bpy)_3{}^{2+}/Ru(bpy)_3{}^{+}$, $BTD^0/BTD^{\bullet-}$, $NB^0/NB^{\bullet-}$, $DNB^0/DNB^{\bullet-}$, $DNB^{\bullet-}/DNB^{2-}$, $TMBQ^0/TMBQ^{\bullet-}$, $MV^{2+}/MV^{\bullet+}$, and $BQ^{\bullet-}/BQ^{2-}$) having the formal potentials ($E^{0'}$ values) more negative than the PZC. CVACO was largely dependent on the concentrations of redox species and TEAP; for example, in the case of BTD the intensity of CVACO increased with increasing concentration, and CVACO ceased at high concentrations of TEAP (≥0.5 M). Furthermore, CVACO was not observed for the $BQ^0/BQ^{\bullet-}$ redox couple having $E^{0'}$ (= −0.31 V) near the PZC, and a pronounced cathodic maximum was observed for the $TCNQ^{\bullet-}/TCNQ^{2-}$ redox couple with $E^{0'}$ (= −0.16 V) more positive than the PZC. These observations and the factors governing the CVACO are discussed on the basis of the theory presented for the polarographic maxima of the first kind. The observed CVACO and the cathodic maximum obtained for the $TCNQ^{\bullet-}/TCNQ^{2-}$ redox couple could be explained in terms of the so-called streaming effect.

Introduction

Recently, our group has reported cyclic voltammetric anodic current oscillation (CVACO) at a hanging mercury drop electrode (HMDE; Figure 1A) based on the redox reaction of the molecular oxygen (O_2)/superoxide ion ($O_2{}^{\bullet-}$) couple in aprotic media.[1−4] The probable causes of this oscillation have been pointed out as follows: (i) the movement of a mercury electrode and its adjoining solution resulting from an inhomogeneous polarization of the electrode (in this case the downward streaming) and (ii) the formation−destruction of a passive film of mercury compounds [e.g., $Hg_2(O_2{}^{\bullet-})_2$] on the electrode surface. However, the mechanism of this oscillation remains uncertain.

Thus far, several research groups have also reported a similar CVACO at a HMDE based on the redox reactions of organic substances[5−8] and metal complex.[9] Santhanam and Bard[5] have suggested that the origin of CVACO observed during the reoxidation of the 9,10-diphenylanthracene anion radical is due to the downward streaming of the Hg surface and its adjoining solution, which leads to the concentration change of redox species in the vicinity of the electrode. According to the consideration of De Levie and Levich,[10,11] this streaming phenomenon is caused by the uneven current density (j) distribution, which arises from the shielding of an upper portion of the Hg drop by the tip of the capillary (Figure 1A) and leads to the uneven potential (E) distribution between the neck and the bottom portions of the Hg drop. Such uneven E distribution finally originates the uneven surface tension (γ) distribution (Figure 1B,C).[5,12] The streaming effects largely depend on whether the oxidation (or reduction) occurs at potentials more negative or positive than the potential of zero charge (PZC). For example, when the electrode reaction occurs at a potential more negative than the PZC, the downward and upward streaming can be expected for the oxidation and reduction processes, respectively (Figure 1C). On the other hand, they should become less, or should be completely absent around the PZC. Thus, in their paper, Santhanam and Bard[5] have also predicted that maximum and stirring behavior could be frequently observed in polarographic oxidations of hydrocarbon and other radicals occurring at potentials more negative than the PZC.

In the present study, we have focused our attention on the current oscillation due to the streaming effect and investigated the oscillation at the HMDE on the basis of the redox reactions of various couples (Figure 2) having their formal potentials ($E^{0'}$ values) more negative or positive than the PZC (i.e., zone I or zone III of the ECC) or around the PZC (i.e., zone II) (Figure 1C). To the best of our knowledge, there has been no report of such a systematic and comprehensive study on the prediction of Santhanam and Bard[5] regarding the polarographic streaming, which induces the current oscillation.

* Author to whom correspondence should be addressed (telephone +81-45-9245404; fax +81-45-9245489; e-mail ohsaka@echem.titech.ac.jp).

10.1021/jp046421a CCC: $27.50 © 2004 American Chemical Society
Published on Web 11/23/2004

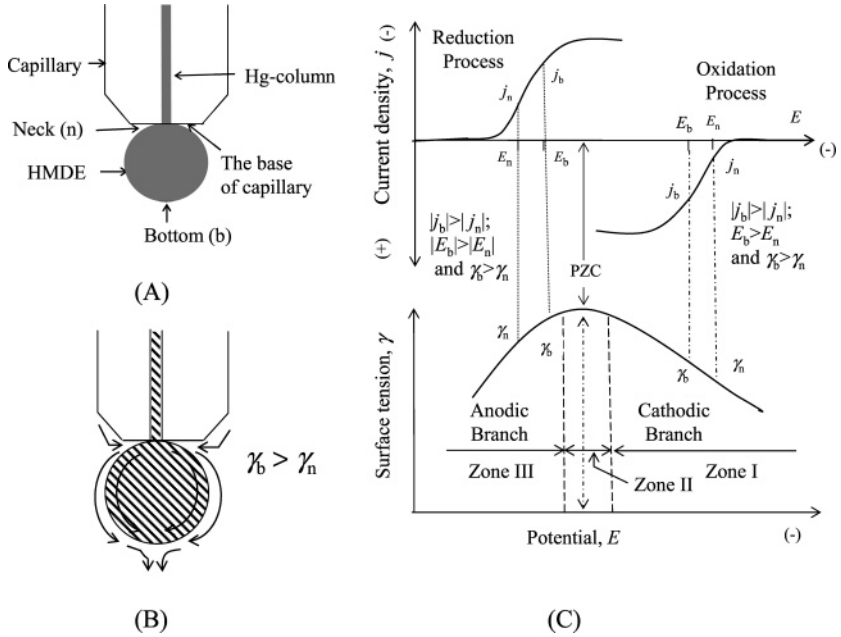

Figure 1. Schematic representation of (A) the cross-section of a hanging mercury drop electrode (HMDE), (B) downward streaming of Hg and its adjoining solution, and (C) an electrocapillary curve (ECC) and the electrochemical processes (i.e., reduction and oxidation). E_n, j_n, and γ_n are the potential, current density, and surface tension at the neck of the drop, respectively; E_b, j_b, and γ_b refer to the bottom of the drop. Zones I and III correspond to the potential regions more negative and positive than the PZC, respectively, and zone II is around the PZC.

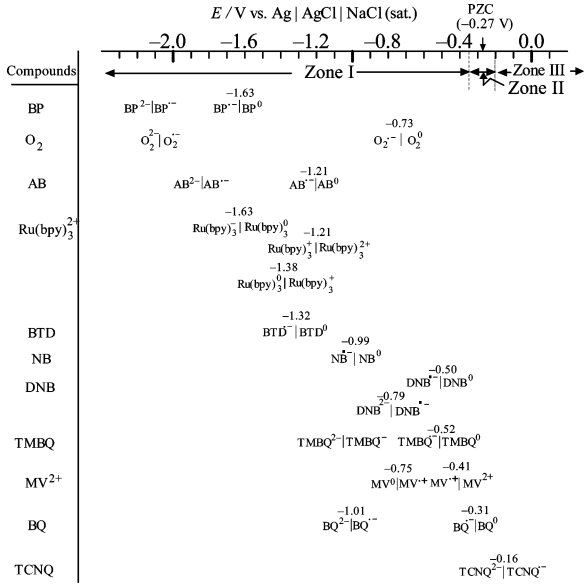

Figure 2. Representation of formal potentials of various redox couples in three zones of the ECC. The value on each redox couple represents its formal potential.

Experimental Section

Reagents. Dimethyl sulfoxide (DMSO) solvent and tetraethylammonium perchlorate (TEAP) as electrolyte were purchased from Kanto Chemical Co. Inc. Prior to use, the solvent was dried by activated molecular sieve (4A 1/16, Wako Pure Chemicals Industries). 1,4-Benzoquinone (BQ), nitrobenzene (NB), azobenzene (AB), and benzophenone (BP) were purchased from Kanto Chemical Co. Inc. 2,3,5,6-Tetramethylbenzoquinone (TMBQ), 2,1,3-benzothiadiazole (BTD), 1,4-dinitrobenzene (DNB), and tris(2,2′-bipyridine)ruthenium(II) dichloride hexahydrate [$Ru(bpy)_3^{2+}$] were commercially available from Aldrich, and methyl viologen dichloride tetrahydrate (MV^{2+}) and 7,7,8,8-tetracyanoquinodimethane (TCNQ) were purchased from Tokyo Kasei Co. Ltd. All of the chemicals were of reagent grade and used without further purifications.

Apparatus and Procedures. Electrochemical experiments were carried out in a conventional two-compartment, three-electrode cell with a hanging mercury drop electrode [HMDE; model CGME 900, Bioanalytical Systems, Inc. (BAS); area = 0.018 cm^2] or glassy carbon (GC; diameter = 1.0 mm) working electrode, a sodium chloride saturated silver|silver chloride [Ag|AgCl|NaCl (sat.)] reference electrode, and a spiral platinum (Pt) wire auxiliary electrode. The electrode cleaning procedures including the purification of metallic Hg by distillation have been described in our previous paper.[4] Each experiment was done with a freshly formed Hg drop as HMDE or with a freshly polished GC electrode. The reference electrode was placed in a glass beaker containing a NaCl-saturated aqueous solution, and this compartment was connected to the cell solution via a salt bridge filled with the electrolytic solution of interest.

The electrocapillary curve (ECC) was determined with a homemade natural dropping Hg electrode in an electrochemical cell with the same arrangement of reference and counter electrodes described above. In the ECC experiment, the Hg drop was allowed to fall through the capillary [the flow rate of Hg (m) = 1.26 mg s^{-1} and the drop time (t) = 4.9 s at the height of Hg head (h) = 79 cm in DMSO solution containing no supporting electrolyte] under different applied potentials. The lifetime of a drop (i.e., drop time) was estimated as an average by counting the total time required for 10 drops at a certain applied potential and then dividing the total time by 10. The measurement at each applied potential was repeated three times to confirm the reproducibility in the obtained drop time. In a similar way, the drop time was determined in the potential range of 0.2 to −1.0 V at potential intervals of 0.1 or 0.05 V. The cyclic voltammetric measurements and the control of the potential during the ECC measurement were performed with a computer-controlled electrochemical system (model 50W, BAS).

The electrochemical impedance spectroscopic (EIS) measurements were done using a Solartron SI 1260 impedance/gain-

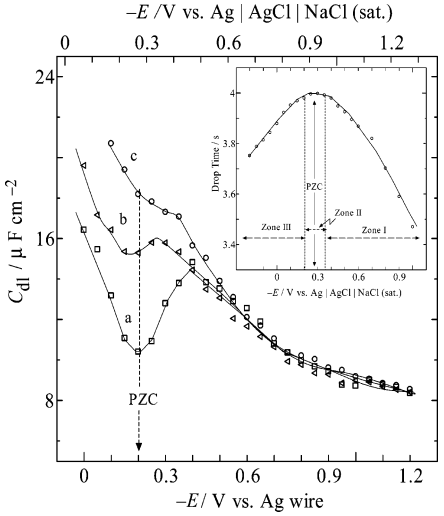

Figure 3. Capacitance (C_{dl}) versus potential (E) curves obtained from the data of impedance measurements, which were carried out at HMDE in DMSO solutions containing various concentrations of TEAP: (a) 0.01, (b) 0.05, and (c) 0.1 M. (Inset) Experimentally determined electrocapillary curve in DMSO solution containing 0.1 M TEAP.

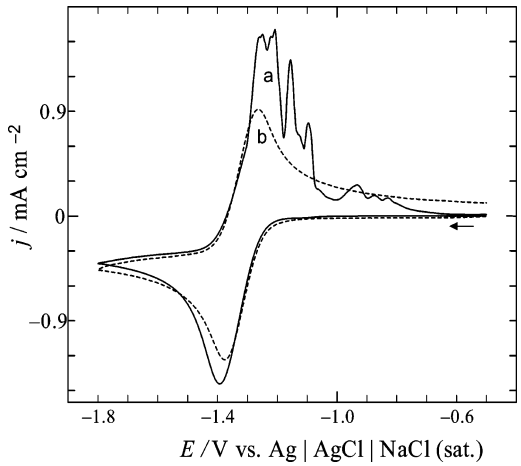

Figure 4. CVs obtained for 5.0 mM BTD at HMDE (a) and GC electrode (b) in a DMSO solution containing 0.1 M TEAP. Potential scan rate: 0.1 V s^{-1}.

phase analyzer combined with a Solartron SI 1287 electrochemical interface. A silver (Ag) wire was used as a quasi-reference electrode instead of the Ag|AgCl|NaCl (sat.) reference electrode by dipping a freshly polished Ag wire into the cell solution to minimize the electrical noise that arose in the use of salt bridge for the Ag|AgCl|NaCl (sat.) reference electrode. The impedance measurement data were obtained at a constant frequency (f) of 1 kHz by scanning the electrode potential (i.e., DC potential) from 0 to −1.2 V at a scan rate of 5 mV s^{-1}, and then the AC potential with 5 mV peak-to-peak amplitude was superimposed on the DC potential. From the impedance measurement data, the values of capacitance (C_{dl}) were calculated according to the equation $-Z'' = 1/(2\pi f C_{dl})$, where Z'' is the imaginary component of impedance (the details have been discussed in ref 13). The value of PZC in DMSO solution containing TEAP was estimated from the C_{dl} versus E curves. To quote the obtained PZC value with respect to the Ag|AgCl|NaCl (sat.) reference electrode, cyclic voltammograms (CVs) for the $O_2/O_2^{\bullet-}$ redox couple were recorded at the HMDE in a DMSO solution containing 0.1 M TEAP at a potential scan rate of 0.1 V s^{-1} using separately Ag wire and Ag|AgCl|NaCl (sat.) electrode as reference electrodes. The peak potential obtained for reduction of O_2 to $O_2^{\bullet-}$ using a Ag wire quasi-reference electrode was found to be more positive by ∼70 mV with a reproducibility of ±10 mV than that obtained using the Ag|AgCl|NaCl (sat.) reference electrode. Thus, the value of PZC was quoted with respect to the Ag|AgCl|NaCl (sat.) reference electrode. In all of the measurements, O_2 gas or N_2 gas was bubbled directly into the cell solutions to obtain their saturated solutions and flushed over the cell solutions during the measurements. All of the experiments were carried out at room temperature (25 ± 2 °C).

Results

Measurements of ECC and PZC of HMDE in DMSO Solution. The so-called three zones in the hypothetical ECC shown in Figure 1C were recognized by constructing an experimental ECC and evaluating the value of PZC. The ECC shown in the inset of Figure 3 was measured using a dropping mercury electrode in a DMSO solution containing 0.1 M TEAP. The drop time versus E curve shows a maximum at a potential of ca. −0.30 V versus Ag|AgCl|NaCl (sat.), and theoretically this observed value of potential corresponds to the PZC.[13] In addition, the EIS measurements were carried out to confirm the PZC value that was obtained in the classical electrocapillary experiment. Figure 3 shows C_{dl} versus E curves obtained at HMDEs in DMSO solutions containing various concentrations of TEAP. At a low concentration of TEAP (e.g., 0.01 M) as shown in Figure 3a the minimum value of capacitance was observed at a potential of −0.20 V versus Ag wire, corresponding to the PZC.[13] Here the value of PZC was quoted with respect to the Ag|AgCl|NaCl (sat.) reference electrode and was found to be −0.27 V. This value is comparable to the literature value of −0.30 V versus SCE in a DMSO solution containing $NaClO_4$.[14] Thus, for the sake of convenience, the potential ranges of zones I, II, and III on the ECC were assigned to more negative than −0.35 V, −0.2 to −0.35 V, and more positive than −0.2 V, respectively.

Typical CVACO at HMDE. Figure 4 shows the typical CVs obtained for the redox reaction of 5.0 mM BTD at a GC electrode and a HMDE in a DMSO solution containing 0.1 M TEAP. The CV obtained at the GC electrode showed well-defined reduction and reoxidation peaks at potentials of −1.37 and −1.28 V versus Ag|AgCl|NaCl (sat.), respectively (Figure 4b). These observed peaks correspond to the one-electron reduction of BTD to its pink anion radical ($BTD^{\bullet-}$) and the reoxidation of $BTD^{\bullet-}$ to BTD.[15,16] The CV obtained at HMDE (Figure 4a) showed the oxidation accompanied by current oscillation. Furthermore, the cathodic peak current obtained at the HMDE was found to be slightly larger than that obtained at the GC electrode. During the cyclic voltammetric measurements, in addition, we also found that in the forward potential scan, BTD was reduced to form a pink $BTD^{\bullet-}$ around the HMDE[15] and that in the backward potential scan the solution containing the colored species was vigorously stirred and then the anodic current oscillation occurred. The $E^{0'}$ obtained for the BTD/$BTD^{\bullet-}$ redox couple (i.e., ca. −1.32 V) is more negative than the PZC, and thus the increase in the cathodic peak current and the anodic current oscillation at the HMDE can be attributed to the polarographic streaming phenomena (Figure 1B,C).[5,10−12]

Effect of Concentration of Redox Species on CVACO. Figure 5 shows the CVs obtained for the consecutive redox reaction of DNB at the HMDE in a DMSO solution containing 0.1 M TEAP. The CVs consisted of two consecutive reduction peaks for the two-step reduction of DNB to $DNB^{\bullet-}$ and $DNB^{\bullet-}$ to DNB^{2-}, and the corresponding two reoxidation peaks of

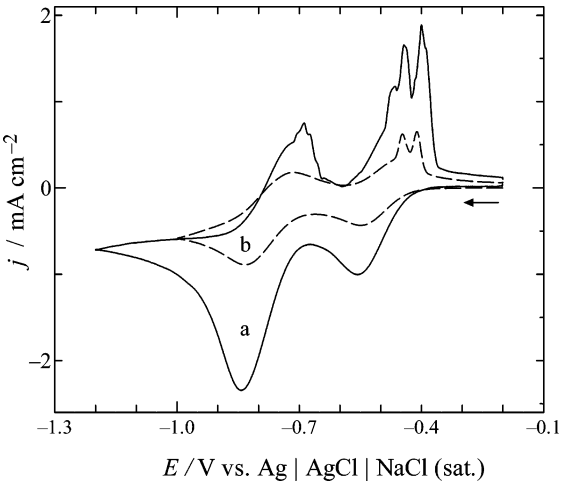

Figure 5. CVs obtained for (a) 5.0 and (b) 2.0 mM DNB at HMDE in DMSO solutions containing 0.1 M TEAP. Potential scan rate: 0.1 V s^{-1}.

TABLE 1: Electrochemical and Current Oscillatory Data of Various Redox Couples in DMSO Solutions Containing 0.1 M TEAP

com-pound[a]	E_p^a/ V[b]	E_p^c/ V[b]	$E^{0'}$/ V[b]	zone[d]	redox couple (ox/red)	current oscillation[e]
BP	−1.59	−1.68	−1.63	I	neutral/anion radical	+
	irr[c]	−2.13		I	anion radical/dianion	irr
O_2	−0.70	−0.76	−0.73	I	neutral/anion radical	+
	irr	−1.86		I	anion radical/dianion	irr
AB	−1.16	−1.26	−1.21	I	neutral/anion radical	+
	irr	−1.84		I	anion radical/dianion	irr
Ru-$(bpy)_3^{2+}$	−1.18	−1.24	−1.21	I	dication/monocation	+
	−1.35	−1.41	−1.38	I	monocation/neutral	−
	−1.60	−1.67	−1.63	I	neutral/monoanion	−
BTD	−1.28	−1.37	−1.32	I	neutral/anion radical	+
NB	−0.94	−1.04	−0.99	I	neutral/anion radical	+
DNB	−0.46	−0.55	−0.50	I	neutral/anion radical	+
	−0.74	−0.84	−0.79	I	anion radical/dianion	+
TMBQ	−0.49	−0.56	−0.52	I	neutral/anion radical	+
	irr	−1.17		I	anion radical/dianion	irr
MV^{2+}	−0.38	−0.44	−0.41	I	dication/cation radical	+
	−0.72	−0.79	−0.75	I	cation radical/neutral	−
BQ	−0.26	−0.36	−0.31	II	neutral/anion radical	−
	−0.96	−1.07	−1.01	I	anion radical/dianion	+
TCNQ	−0.13	−0.20	−0.16	III	anion radical/dianion	cathodic max

[a] Abbreviations: BP, benzophenone; O_2, molecular oxygen; AB, azobenzene; $Ru(bpy)_3^{2+}$, tris(2,2′-bipyridine)ruthenium(II) chloride; BTD, 2,1,3-benzothiadiazole; NB, nitrobenzene; DNB, 1,4-dinitrobenzene; TMBQ, 2,3,5,6-tetramethylbenzoquinone; MV^{2+}, methyl viologen dichloride; BQ, benzoquinone; TCNQ, 7,7,8,8-tetracyanoquinodimethane. [b] E_p^a and E_p^c indicate the values of anodic and cathodic peak potentials, respectively, which were taken from the CVs obtained for the individual compounds with GC working electrode at a potential scan rate of 0.1 V s^{-1}. $E^{0'}$ is the formal potential and was estimated as the average of the values of E_p^a and E_p^c for each redox couple. All of the potentials were measured and are quoted with respect to a Ag|AgCl|NaCl (sat.) reference electrode. [c] "irr" indicates that a redox reaction is electrochemically irreversible and that the anodic peak potential and current oscillation are not observed. [d] Zones I, II, and III represent the potential regions of < -0.35 V, -0.35 to -0.2 V and > -0.2 V versus Ag|AgCl|NaCl (sat.), respectively, and the individual redox couples are grouped into these zones depending on the $E^{0'}$ values (see Figure 1C). [e] "+" and "−" represent the presence and absence of current oscillation, respectively.

DNB^{2-} to $DNB^{\bullet-}$ and $DNB^{\bullet-}$ to DNB (Table 1). The anodic current oscillation was observed in the reoxidation processes as in the oxidation of $BTD^{\bullet-}$ (Figure 4). Interestingly, we could observe the current oscillation in both of the consecutive reoxidation peaks when the concentration of DNB was 5.0 mM, whereas the oscillation was observed only in the reoxidation peak of $DNB^{\bullet-}$ when its concentration was 2.0 mM. In the present case, both redox reactions occur in zone I (Table 1 and Figure 3), and therefore the current oscillation can be expected to occur in both reoxidation processes. The effect of the concentration of the redox species on CVACO in a single redox couple can also be seen in Figures 4a and 6a, where an enhanced CVACO was observed when the concentration of BTD was 5.0 mM and it was attenuated at 1.0 mM. It has been reported that the concentration of the redox species affects the streaming of the Hg surface;[5,12] that is, the streaming of the Hg surface and its adjoining solution increases as the concentration of the redox species increases. The present observations are in accordance with the experimental results reported previously[1−5] as well as the theoretical prediction[12,17,18] that lowering the concentration of the redox species attenuates CVACO.[5] Thus, the concentration of the redox species has a great influence on the oscillation and CVACO takes place in both of the consecutive redox processes only when the concentration of the redox species is sufficiently high. It is also mentioned that in the case of DNB the second reduction peak current is significantly larger than the first one, although the number of electrons involved in each step is identical, that is, one (see especially Figure 5a). This unusual observation has been claimed to result from the streaming of the Hg surface as well.[19,20]

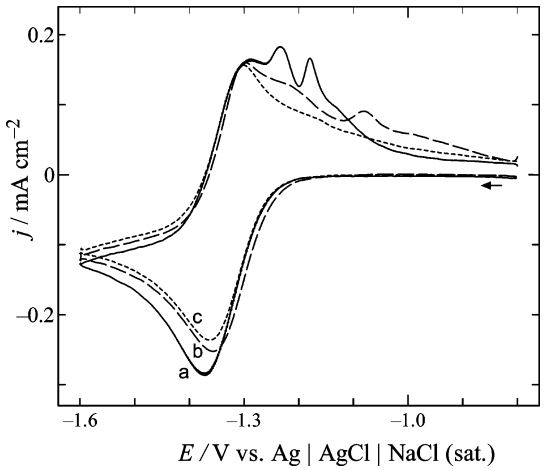

Figure 6. CVs obtained for 1.0 mM BTD at HMDE in DMSO solutions containing various concentrations of TEAP: (a) 0.1, (b) 0.3, and (c) 0.5 M. Potential scan rate: 0.1 V s^{-1}.

Effects of Supporting Electrolyte on CVACO. Figure 6 shows the CVs obtained for 1.0 mM BTD in DMSO solutions containing various concentrations of TEAP. When the concentration of TEAP was 0.1 M, the reoxidation wave was observed with current oscillation (Figure 6a), which is similar to the case of 5.0 mM BTD shown in Figure 4. In this case, the attenuated oscillation can be ascribed to the lower concentration of BTD. Furthermore, this oscillation decayed with increasing concentration of TEAP, and it was completely damped when the TEAP concentration was 0.5 M (discussed later).

Oscillatory Phenomenon Based on Various Redox Reactions at HMDE. For the purpose of the present study, we chose various redox couples with different $E^{0'}$ values that belong to different zones on the ECC (Figure 1C). The CVs of 20 redox couples at the HMDE and the GC electrode were measured in DMSO solutions containing 0.1 M TEAP. In almost all cases, we observed CVACO at the HMDE, whereas no CVACO was observed at the GC electrode. The results of cyclic voltammetric measurements are summarized in Table 1. The values of $E^{0'}$

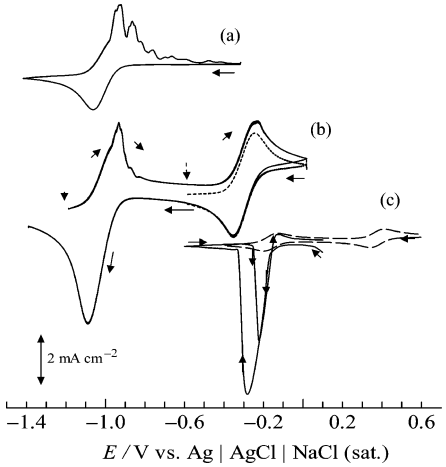

Figure 7. Typical CVs obtained for 2.0 mM NB (a), 5.0 mM BQ (b), and 1.0 mM TCNQ (c) at HMDE in DMSO solutions containing 0.1 M TEAP. The direction of the potential scan is marked by arrows. In the CVs of (b) the downward arrows indicate the initial potential, at which the potential was held for 10 s. The solid and dashed lines in (c) represent the CVs obtained at HMDE and GC electrode, respectively. Potential scan rate: 0.1 V s^{-1}.

for the compounds given in Table 1 agree well with those reported in the literature.[1−4,13,15,16,21,22] The data in Table 1 are also represented in Figure 2 in such a way that we can see simply the possibility of CVACO based on each redox couple from a simple inspection of the position of $E^{0'}$ with respect to the PZC.

CVs Obtained for the Redox Reactions of Various Neutral Organic Compounds at the HMDE in Three Zones on the ECC. Figure 7 represents the typical CVs obtained for the redox reactions of NB, BQ, and TCNQ at the HMDE in DMSO solutions containing 0.1 M TEAP. The CV obtained for NB (Figure 7a) shows a well-defined reduction peak at ca. −1.04 V (i.e., in zone I), whereas its reoxidation peak appears with the oscillation, being essentially similar to the case of BTD (Figure 4a).

The cyclic voltammetric response of BQ shows two redox waves with $E^{0'}$ values of ca. −0.3 and ca. −1.0 V. Assuming that the potential range of zone II is ca. −0.2 to −0.35 V, the $E^{0'}$ values of the first and second redox couples would be in zones II and I on the ECC, respectively. Thus, from Figure 1C, the first and second reoxidation waves can be expected to appear without and with oscillation, respectively. In practice, however, the oscillation did not essentially occur in the first reoxidation wave, and it was hardly observed in the second reoxidation wave either [especially at higher potential scan rates (>0.2 V s^{-1})] when the potential was scanned from 0 to −1.4 and then to 0 V (data are not shown here). However, interestingly, the oscillation appeared, as expected, when the potential scan was started from −1.2 V to the positive direction. Figure 7b shows the CV (solid line) obtained for BQ at the HMDE in a DMSO solution containing 0.1 M TEAP by scanning the potential in the direction of −1.2 → 0 → −1.4 V after the potential had been held at its initial potential, −1.2 V, for 10 s. As the initial potential, −1.2 V, is more negative than that of the second reduction peak of BQ (i.e., −1.07 V), while the potential is held at −1.2 V, BQ is reduced to BQ^{2-} via $BQ^{\bullet-}$ under a diffusion-controlled condition. After the potential had been held at −1.2 V, during the anodic potential scan the electrogenerated BQ^{2-} is oxidized to BQ through two consecutive one-electron oxidation processes (Table 1), and in the reverse cathodic potential scan from 0 to −1.4 V the parent molecule BQ undergoes two consecutive one-electron reductions and finally is reduced to BQ^{2-}. In this case, we found that CVACO was observed only around the second reoxidation peak in zone I (i.e., ca. −0.95 V), whereas the first reoxidation peak in zone II (i.e., −0.23 V) appeared without oscillation. The absence of oscillation in the first redox wave ($E^{0'} = -0.3$ V) was confirmed by another similar experiment, in which the initial potential of −0.6 V was chosen, and the potential was held at −0.6 V for 10 s, and then the potential was scanned in the positive direction. The obtained CV is shown in Figure 7b (dotted line). It is obvious that the reoxidation peak (i.e., ca. −0.25 V) is not accompanied by current oscillation, indicating that the oscillation is absent in zone II.

In the present study, we could not thoroughly investigate the cyclic voltammetric response at the HMDE in zone III because of the anodic dissolution of the Hg electrode itself. Figure 7c shows the CVs obtained for TCNQ at the HMDE (solid line) and the GC electrode (dashed line) in a DMSO solution containing 0.1 M TEAP. Two well-defined one-electron redox waves were observed at the GC electrode, whereas a largely enhanced cathodic peak and an inverted cathodic-like peak were found for the $TCNQ^{\bullet-}/TCNQ^{2-}$ couple during the cathodic and anodic potential scans, respectively. In this case, the reduction peak height obtained at the HMDE was ∼19 times larger than that at the GC electrode. This enormously large peak current[23] observed during the cathodic potential scan would be attributed to the downward streaming phenomenon that can actually occur in zone III (Figure 1C).[1,2,5,12,17,18] It has also been theoretically established that such an unusual cathodic peak appears when the cathodic process proceeds at potentials more negative than the PZC,[17,18] that is, in zone III. Hence, the present observation on the cathodic wave of $TCNQ^{\bullet-}$ is in good agreement with the theoretical consideration, and at the same time this verifies the presence of the downward streaming phenomenon shown in Figure 1B,C. On the other hand, $Hg^{2+}(TCNQ^{\bullet-})_2$ complex salt[24] and $TEA^+(TCNQ^{\bullet-})(TCNQ)$ complex salt[25] (where TEA^+ is tetraethylammonium cation) have been well-known, and therefore the observed inverted peak[8] could be associated with desorption or further reduction of the adsorbed products formed in the reactions between the Hg electrode or the supporting electrolyte cation (i.e., TEA^+) and the electroreduced products of TCNQ.

CVs Obtained for the Redox Reactions of a Positively Charged Metal Complex and an Organic Compound. We found some exceptions in our observations, that is, the absence of oscillation in the CVs obtained for the redox reactions of $Ru(bpy)_3^{2+}$ and MV^{2+}. Figures 8 and 9 show typical CVs obtained for the redox reactions of $Ru(bpy)_3^{2+}$ and MV^{2+}, respectively, in DMSO solutions containing 0.1 M TEAP. The number of observed redox peaks and the values of cathodic and anodic peak potentials (Table 1) for both redox species agree well with those reported in the literature.[13,21,26]

In the case of $Ru(bpy)_3^{2+}$ (Figure 8), the cyclic voltammetric responses of three redox couples were observed, and all of the $E^{0'}$ values belong to zone I (Figure 2). The oscillation was observed only when the potential was scanned in the range where the redox reactions for the $Ru(bpy)_3^{2+}/Ru(bpy)_3^+$, $Ru(bpy)_3^+/Ru(bpy)_3^0$ and $Ru(bpy)_3^0/Ru(bpy)_3^-$ couples took place (Figure 8a). Because all of the redox reactions occur in zone I, from our prediction, the oscillation can be expected to occur in all three reoxidation processes. Contrary to the expectation, however, we found that the oscillation appeared on the first reoxidation wave around −0.8 V only after the observation of the redox reaction of the $Ru(bpy)_3^0/Ru(bpy)_3^-$ couple. This

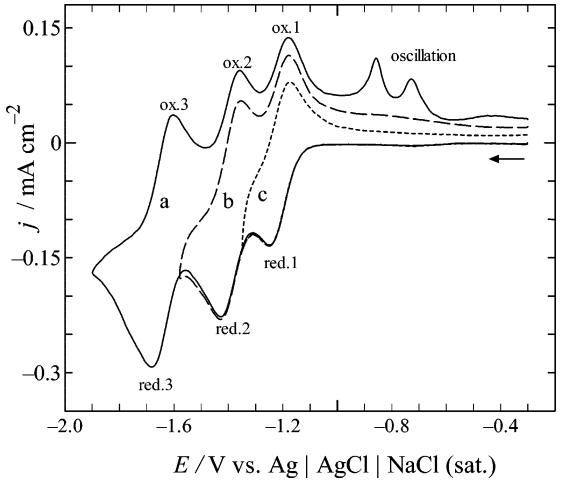

Figure 8. CVs obtained for 1.0 mM $Ru(bpy)_3^{2+}$ at HMDE in a DMSO solution containing 0.1 M TEAP in the different potential range. Reverse potentials: (a) −1.9; (b) −1.6; (c) −1.38 V. Potential scan rate: 0.1 V s^{-1}.

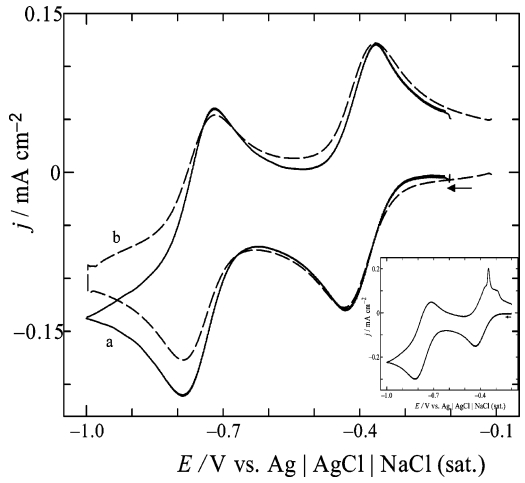

Figure 9. CVs obtained for 1.0 mM MV^{2+} at (a) HMDE and (b) GC electrode in a DMSO solution containing 0.1 M TEAP. (Inset) CV obtained for 1.0 mM MV^{2+} at HMDE in a DMSO solution containing 0.01 M TEAP. Potential scan rate: 0.1 V s^{-1}.

situation seems to be similar to that reported by Guyon et al.[9] They have observed a similar current spike on the anodic wave of CVs obtained for the Ni(II)/Ni(I) salen couple, which includes neutral and negatively charged species, at HMDE in DMF solution. Using double-potential-step chronocoulometry, Guyon et al. have confirmed that the current spike observed on the anodic wave is associated neither with adsorption of redox reaction product on the electrode nor with the oxidation of precipitate formed in the chemical reaction between a cation of the supporting electrolyte and an anionic reaction product on the HMDE surface. Consequently, they have concluded that the observed oscillation would be due to streaming phenomenon rather than adsorption or redox reaction.

Figure 9 represents typical CVs obtained for the redox reaction of 1.0 mM MV^{2+} in a DMSO solution containing 0.1 M TEAP. Two redox waves for $MV^{2+}/MV^{\bullet+}$ and $MV^{\bullet+}/MV^0$ couples were observed without oscillation, even though $E^{0'}$ values of both redox couples[25,26] belong to zone I (Table 1). It has been reported that the intensity of CVACO depends on the concentration of redox species[5] as shown in Figures 4a, 5, and 6a. When we increased the concentration of MV^{2+} to its saturated concentration in DMSO solution (i.e., 1.0 mM), no effect of concentration of MV^{2+} on anodic waves was observed except for the essential increase in the peak current reflecting the increase in the concentration. Furthermore, during the redox reactions of MV^{2+}, where MV^{2+} was reduced to form the corresponding blue cation radical and neutral species and the reduced species were reoxidized to form colorless MV^{2+}, we did not observe the movement of the colored species around HMDE, being different from the case of BTD (Figure 4).

The effect of iodide ion on the current oscillation of the $O_2/O_2^{\bullet-}$ redox couple has been studied, and the use of iodide as the counteranion of the supporting electrolyte has found to suppress the current oscillation completely in an air-saturated DMSO solution containing 0.1 M tetra-*n*-butylammonium iodide.[4] Therefore, whether the current oscillation is suppressed by halide ions or not was also examined in this study. MV^{2+} used here is an organic salt containing the Cl^- ion as counteranion, and we used a 1.0 mM MV^{2+} solution in our experiment. The amount of Cl^- ion (2.0 mM), in this case, does not seem to be sufficient to stop the current oscillation completely because the Cl^- ion is weaker than the I^- ion with respect to the strength of their specific adsorptions onto the Hg surface. Therefore, the lack of observation of CVACO in the case of MV^{2+} is considered not to be due to the influence of Cl^- ion. In addition, we also tried to examine the CVACO of 1.0 mM $Ru(bpy)_3^{2+}$ by adding 4.0 mM tetraethylammonium chloride salt into the solution because this $Ru(bpy)_3^{2+}$ solution contains 2.0 mM Cl^- ion. We found that the addition of the Cl^- ion did not damp the current oscillation. This also verifies that the absence of current oscillation in the case of the redox reactions of MV^{2+} would not be ascribed to the presence of the Cl^- ion.

We can see from Figure 6 that the concentration of supporting electrolyte has a great effect on CVACO; that is, the current oscillation diminishes at higher concentrations of TEAP. The inset of Figure 9 shows the CV obtained for 1.0 mM MV^{2+} in a DMSO solution containing 0.01 M TEAP. In this case the current oscillation was observed for the $MV^{2+}/MV^{\bullet+}$ redox couple, but was absent for the $MV^{\bullet+}/MV^0$ redox couple. This observation is essentially similar to that shown in Figure 5.

Discussion

The data summarized in Table 1 and Figure 2 reveal that CVACO strongly depends on a position of $E^{0'}$ of a redox couple relative to the PZC. That is, CVACO can be observed only for the redox couples having $E^{0'}$ values more negative than the PZC, that is, in zone I, and the more negative $E^{0'}$ is with respect to the PZC, the more intense the oscillation becomes (Figures 4a and 7a), whereas it is attenuated for the redox couple having $E^{0'}$ close to the PZC (Figure 7b). All of these facts, except for the redox couples of MV^{2+} and $Ru(bpy)_3^{2+}$ in which the current oscillation was really observed [but some unexpected results were also obtained (as mentioned above)], can be satisfactorily explained on the basis of the theory presented for the so-called first-kind streaming;[5,10−12] that is, uneven E distribution, or uneven γ distribution on the HMDE surface (i.e., the significant magnitude of the $|\Delta E|$, or $|\Delta\gamma|$) originates the streaming phenomenon of the Hg surface and its adjoining solution (Figure 1B,C).

The oscillation is not observed for the redox couples having $E^{0'}$ near the PZC, that is, in zone II (e.g., Figure 7b), and this can be understood from the fact that the current density (j_n), potential (E_n), and surface tension (γ_n) at the neck portion of the HMDE are almost identical to those at its bottom portion; that is, $|\Delta E|$ and $|\Delta\gamma|$ are actually zero. This situation on the HMDE surface is essentially unfavorable for inducing the streaming (downward or upward) phenomena (Figure 1C).

Hence, the generation of streaming force on the electrode surface seems to be a prerequisite for CVACO in zone I. On the other hand, for the redox couples having $E^{0'}$ values in the potential region more positive than the PZC (i.e., in zone III), the situation is completely the reverse of that just mentioned for the redox couples in zone I; that is, for example, the upward and downward streaming phenomena can be expected for the reduction processes of redox couples in zones I and III, respectively (Figure 1). Thus, the appearance of a sharp cathodic peak in the CV obtained for TCNQ at HMDE (Figure 7c) can be ascribed to the downward streaming phenomenon of the Hg surface characteristic of the reduction process in zone III.

Thus, it is clear that CVACO originates only at the potentials more negative than the PZC (zone I), where the downward streaming of the Hg surface can be expected to occur during an oxidation process (Figure 1B,C). This can also be supported from the effect of the electrolyte (TEAP) concentration on CVACO (Figures 6 and 9). The oscillation is more effectively diminished in the presence of higher concentrations (Figure 6c). This can be explained by considering the fundamental equation of the current−potential relationship

$$\Delta E = R\Delta j \tag{1}$$

where R is the resistance of the solution and ΔE and Δj are the differences in potentials and current densities at different regions of the HMDE (e.g., the neck and bottom portions), respectively. In general, as the concentration of electrolyte increases, R decreases, and consequently ΔE decreases.[5,27] Because $|\Delta\gamma|$ is directly proportional to ΔE in a specified electrolytic solution,[13] $|\Delta\gamma|$ decreases with increasing concentration of electrolyte. The decrease in $|\Delta\gamma|$ weakens the streaming phenomenon and hence stops the oscillation. The present observations are in agreement with the prediction by Santhanam and Bard in 1966.[5]

Conclusions

The CVACO at the HMDE in DMSO has been studied systematically for 20 redox couples of organic compounds and metal complex. CVACO was found to occur only for the redox couples having formal potentials ($E^{0'}$ values) more negative than the PZC (−0.27 V). In addition, CVACO was not observed for the $BQ^0/BQ^{\bullet-}$ redox couple with $E^{0'}$ near the PZC and the $TCNQ^{\bullet-}/TCNQ^{2-}$ redox couple with $E^{0'}$ more positive than the PZC. The obtained results and the origin of CVACO are satisfactorily explained in terms of the so-called streaming phenomenon based on the theory presented for the polarographic streaming maxima of the first kind.

Acknowledgment. The present work was supported financially by Grant-in-Aids for Scientific Research on Priority Areas (No. 417), Scientific Research (No. 12875164), and Scientific Research (A) (No. 10305064) to T.O., from the Ministry of Education, Culture, Sports, Science and Technology of the Japanese government (Monbu-Kagakusho). M.M.I. gratefully acknowledges the government of Japan for a Monbu-Kagakusho scholarship and appreciates the financial support of the KATOH Science Foundation, Japan.

References and Notes

(1) Saha, M. S.; Che, Y.; Okajima, T.; Kiguchi, T.; Nakamura, Y.; Tokuda, K.; Ohsaka, T. *J. Electroanal. Chem.* **2001**, *496*, 61.
(2) Saha, M. S.; Okajima, T.; Ohsaka, T. *J. Phys. Chem. B* **2002**, *106*, 4457.
(3) Che, Y.; Okajima, T.; Nakamura, Y.; Tokuda, K.; Ohsaka, T. *Chem. Lett.* **1998**, 97.
(4) Islam, M. M.; Saha, M. S.; Okajima, T.; Ohsaka, T. *J. Electroanal. Chem.*, in press.
(5) Santhanam, K. S. V.; Bard, A. J. *J. Am. Chem. Soc.* **1966**, *88*, 2669.
(6) Chen, T.-Y. R.; Anderson, M. R.; Peters, D. G. *J. Electroanal. Chem.* **1987**, *222*, 257.
(7) Aravamuthan, S.; Kalidas, C.; Venkatachalam, C. S. *J. Electroanal. Chem.* **1984**, *171*, 293.
(8) Ginzburg, G.; Becker, J. Y.; Lederman, E. *Electrochim. Acta* **1981**, *26*, 851.
(9) Guyon, A. L.; Klein, L. J.; Goken, D. M.; Peters, D. G. *J. Electroanal. Chem.* **2002**, *526*, 134.
(10) De Levie, R. *J. Electroanal. Chem.* **1965**, *9*, 331.
(11) Levich, V. G. *Physicochemical Hydrodynamics*; Prentice Hall: New York, 1962; p 577.
(12) Bauer, H. H. In *Electroanalytical Chemistry*; Bard, A. J., Ed.; Dekker: New York, 1975; Vol. 8, p 169.
(13) Bard, A. J.; Faulkner, L. R. *Electrochemical Methods, Fundamentals and Applications*; Wiley: New York, 1980.
(14) Payne, R. *J. Am. Chem. Soc.* **1967**, *89*, 489.
(15) Islam, M. M.; Okajima, T.; Ohsaka, T. *Electrochem. Commun.* **2004**, *6*, 556.
(16) Atherton, N. M.; Ockwell, J. N. *J. Chem. Soc. (A)* **1967**, 771.
(17) Aogaki, R.; Kitazawa, K.; Fueki, K.; Mukaibo, T. *Electrochim. Acta* **1978**, *23*, 867.
(18) Aogaki, R.; Kitazawa, K.; Fueki, K.; Mukaibo, T. *Electrochim. Acta* **1978**, *23*, 875.
(19) Becker, J. Y.; Ginzburg, G.; Willner, I. *J. Electroanal. Chem.* **1980**, *108*, 355.
(20) Islam, M. M.; Okajima, T.; Ohsaka, T. Manuscript in preparation.
(21) Mann C. K.; Barnes, K. K. *Electrochemical Reactions in Nonaqueous Systems*; Dekker: New York, 1970.
(22) Izutsu, K. *Electrochemistry in Nonaqueous Solutions*; Wiley-VCH: Weinheim, Germany, 2002.
(23) Giordano, M. C.; López, B. A.; Sereno, R. *J. Electroanal. Chem.* **1979**, *101*, 39.
(24) Fadly, M.; El-Gandoor, M. A.; Sawaby, A. *J. Mater. Sci.* **1992**, *27*, 1235.
(25) Melpy, L. R.; Harder, R. J.; Hertler, W. R.; Mahler, W.; Benson, R. E.; Mochel, W. E. *J. Am. Chem. Soc.* **1962**, *84*, 3374.
(26) Kim, J. Y.; Lee, C.; Park, J. W. *J. Electroanal. Chem.* **2001**, *504*, 104.
(27) Okinaka, Y.; Kolthoff, I. M.; Murayama, T. *J. Am. Chem. Soc.* **1965**, *87*, 423.